Supporting Information

Recellularization and Integration of Dense Extracellular Matrix by Percolation of Tissue Microparticles

Jeanne E. Barthold[1], Brittany M. St. Martin[1], Shankar Lalitha Sridhar[1], Franck Vernerey[1], Stephanie Ellyse Schneider[1], Alexis Wacquez[1], Virginia Ferguson[1,2], Sarah Calve[1,3], Corey P. Neu[1,2,]*

[1] Paul M. Rady Department of Mechanical Engineering, University of Colorado Boulder, Boulder, CO
[2] BioFrontiers Institute, University of Colorado Boulder, Boulder, CO
[3] Weldon School of Biomedical Engineering, Purdue University, West Lafayette, IN

Table S1. Transwell cellular migration data from select cell types. References are provided at the end of the Supplemental Information.

Cell Type	Transwell pore (μm)	Nuclear Diameter	10% Diameter	Pore/10% Nuclear Diameter	% cells migrate	time (hours)	Chemo attractant
Chondrocyte	8 [46]	5	0.5	16.0	11% [46]	24	PDGF
MSC	8 [46]	6	0.6	13.3	13% [46]	24	PDGF
Fibrochondrocyte	3 [47]	9 [47]	0.9	3.3	0% [6]	16	PDGF
Fibrochondrocyte	5 [47]	9 [47]	0.9	5.6	20% [6]	16	PDGF
Fibrochondrocyte	8 [47]	9 [47]	0.9	8.9	50% [6]	16	PDGF
Myoblasts	8 [48]	10 [49]	1	8.0	10% [48]	24	PDGF
Epithelial Cell	10[50]	5[50]	0.5	20.0	83% [50]	24	10% FBS
Epithelial Cell	8[50]	5[50]	0.5	16.0	65% [50]	24	10% FBS
Epithelial Cell	7[50]	5[50]	0.5	10.0	50% [50]	24	10% FBS
Neutrophil	0.45	3	0.3	1.5	0% [51]	20	IL8
Neutrophil	3 [51]	3 [51]	0.3	10.0	10% [51]	20	IL8

Table S2. *In vivo* migration data from select cell types. References are provided at the end of the Supplemental Information.

Tissue or System	Cell type	Nucleus diameter (µm)	*In Vivo* Pore size (µm)	Pore size/ Nucleus	Pore size/10 % Nucleus	Migration rate (µm /min)	Notes on Migration Rate
Skin	Fibroblast	7 [52]	2 [52]	0.28	2.86	0.915 [53]	3D collagen
Breast	mammary epithelial cell	4.9 [54]	5 [50]	1.02	10.23	1.5 [55]	2D on collagen
Meniscus	Fibrochondrocyte	9 [6]	0.01 [56]	0.001	0.01	0.0014 [47]	Native tissue slice
Muscle	Smooth muscle cell	5 [57]	0.44 [57]	0.088	0.88	0.7 [58]	2D on Polyacryl.
Muscle	Satellite cells	4 [59]	0.44 [57]	0.11	1.1	0.833 [59]	
Cartilage	Chondroctye	5 [35]	0.006 [60]	0.0012	0.012	0.027 [61]	
Stem Cell	MSC	7 [62]	6 [63]	0.86	8.57	1 [64]	
Bone	Osteocyte	2 [63]	0.2 [63]	0.1	1	0.002	
Adipose	Adipocytes	5 [65]	10 [66]	2	20	0.33 [65]	
Immune	Leukocyte	6 [4]	0.8 [4]	0.13	1.33	10 [4]	3D collagen
Immune	Tcells	3.1 [4]	0.8 [4]	0.26	2.59	11 [67]	*In vivo* lymph
Cancer	Breast Sarcoma Cell	7.7 [4]	10 [4]	1.30	13.03	0.33 [4]	3D collagen
Immune	Neutrophil	2.5 [4]	0.8 [4]	0.32	3.17	11 [4]	3D collagen

Calculation S1: Calculation of percolation threshold from Generalized Effective Medium Theory. In this section, we provide the mathematical equation corresponding to the Generalized Effective Medium Theory [18] that were used to fit the effective compressive modulus of the composite material.

The effective mechanical properties of composite materials are typically described using the volume fractions and the corresponding mechanical properties of the constituents. In a two-constituent system, the overall effective compressive modulus E_{eff} is influenced by the spatial distribution and connectivity of the inclusions of each constituent. Multiple theories on percolation of the inclusions have been introduced to model this behavior. The generalized effective medium theory (GEM) has been found to be the most robust as it can provides a general approach to incorporate differences in percolation thresholds arising from the geometry of the inclusions. Let us denote material 1 as the hydrogel with compressive modulus E_1 and material 2 as the native cartilage with compressive modulus E_2 whose pieces are encapsulated in the sample. Let f denote the volume fraction of cartilage in the entire sample such that $1-f$ denotes the volume fraction of hydrogel. The effective compressive modulus E_{eff} can be determined by solving the following equation

$$(1-f)\frac{E_1^{1/s}-E_{eff}^{1/s}}{E_1^{1/s}+(f_c^{-1}-1)E_{eff}^{1/s}}+f\frac{E_2^{1/t}-E_{eff}^{1/t}}{E_2^{1/t}+(f_c^{-1}-1)E_{eff}^{1/t}}=0 \quad (1)$$

where f_c is the percolation threshold for the volume fraction of cartilage. The terms s and t are the characteristic exponents corresponding to a universal scaling law for effective properties at volume fractions near the percolation threshold f_c. These exponent s captures the sharpness of the transition of the effective modulus from E_1 when $f \ll f_c$ while the exponent t captures the transition to a value of effective modulus of E_2 when $f_c < f \to 1$. The figure below shows two plots of the effective modulus E_{eff} as a function of the volume fraction f for different values of s and t.

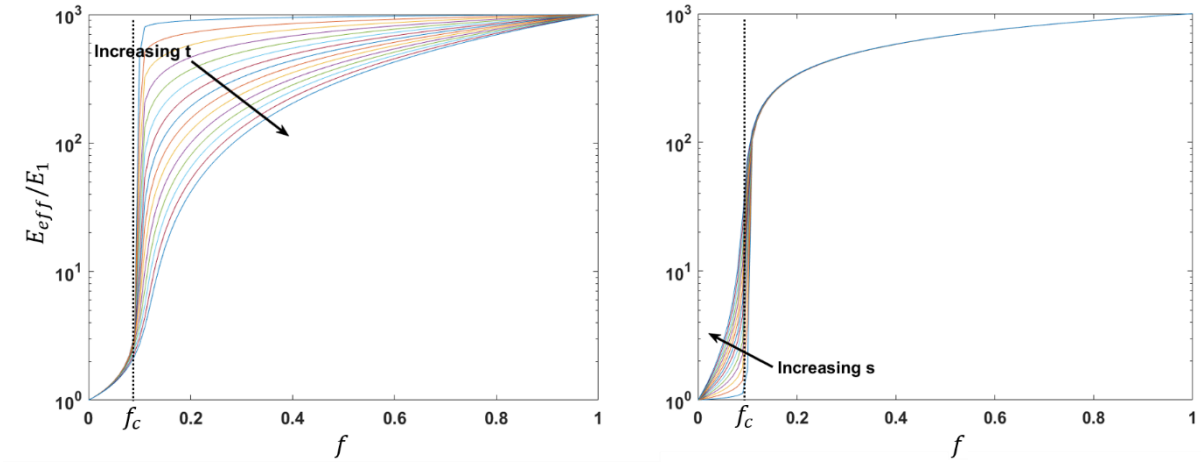

Figure S1. Plots of the ratio of effective compressive modulus E_{eff}/E_1 predicted by the GEM theory as a function of the volume fraction f of cartilage. The difference in the sharpness of transition from the modulus of the hydrogel E_1 to that of cartilage E_2 is illustrated with changes in the exponents s and t.

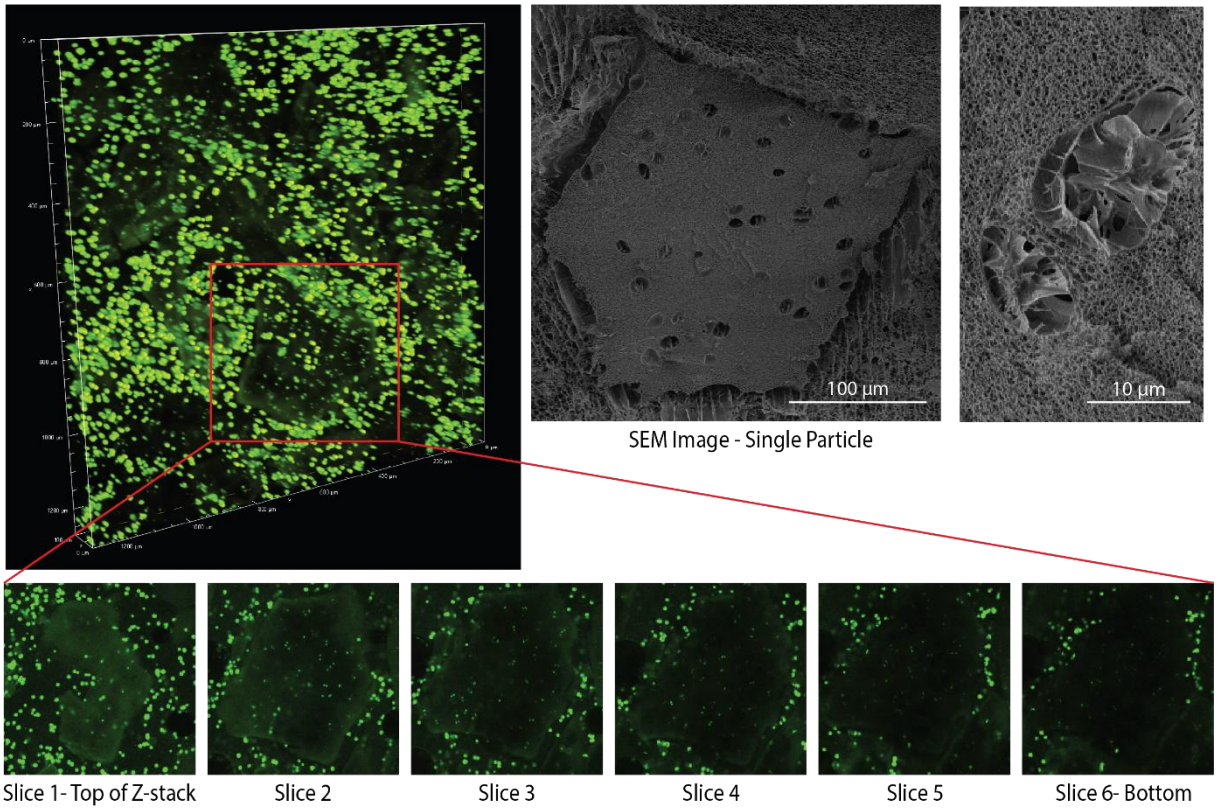

Figure S2. Confocal z-stack imaging of a section of the tissueclay construct with CFSE stained cells, demonstrates cellular migration into the particles confirming migration rather than just cellular attachment to the surface. Additionally, Scanning Electron Microscopy Images of acellular tissue particles illustrate that regions previously formed for chondrons are 10-15 µm in diameter, providing several regions of much larger pores than the surrounding cartilage extracellular matrix to enable cell migration.

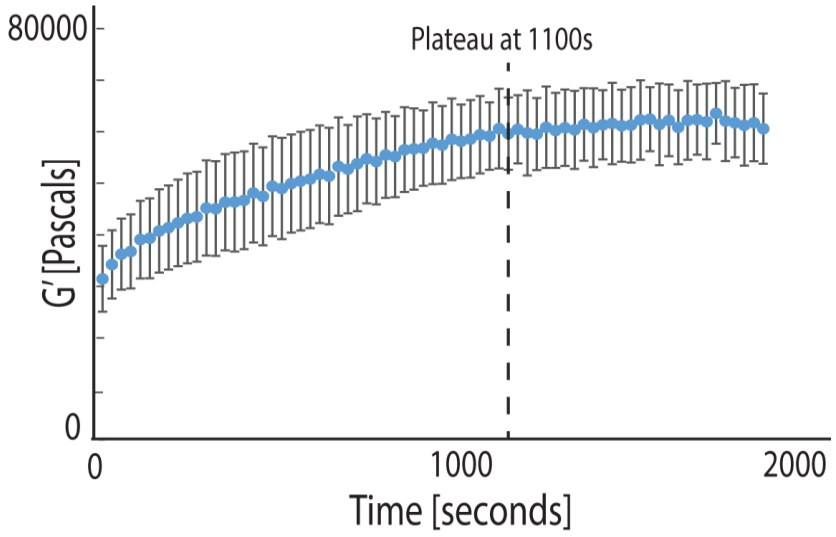

Figure S3. *Tissue clay* hydrogel crosslinks in ~15 minutes, as demonstrated using rheological testing (*n*=3). **The rheological data shown was obtained using an oscillation procedure with time sweep with a rheometer (AR-G2, TA Instruments), with metal plates (boundaries) set to 37 ℃. The time sweep took place at a constant frequency of 0.5 rads/sec and 0.5% strain (confirmed to be in the viscoelastic region with a frequency sweep of the HA/PEGDA material [26]) for a total of 30 minutes. The shear modulus over time was obtained using 25 mm aluminum flat discs with an 800µm separation gap to confirm crosslinking and evaluate the time to crosslinking of the polymer matrices present. Low viscosity mineral oil was applied to the outer surface of the scaffolds to maintain moisture in the hydrogels throughout testing. Curves for three independent samples were averaged and evaluated to determine the plateau (or formation) point.**

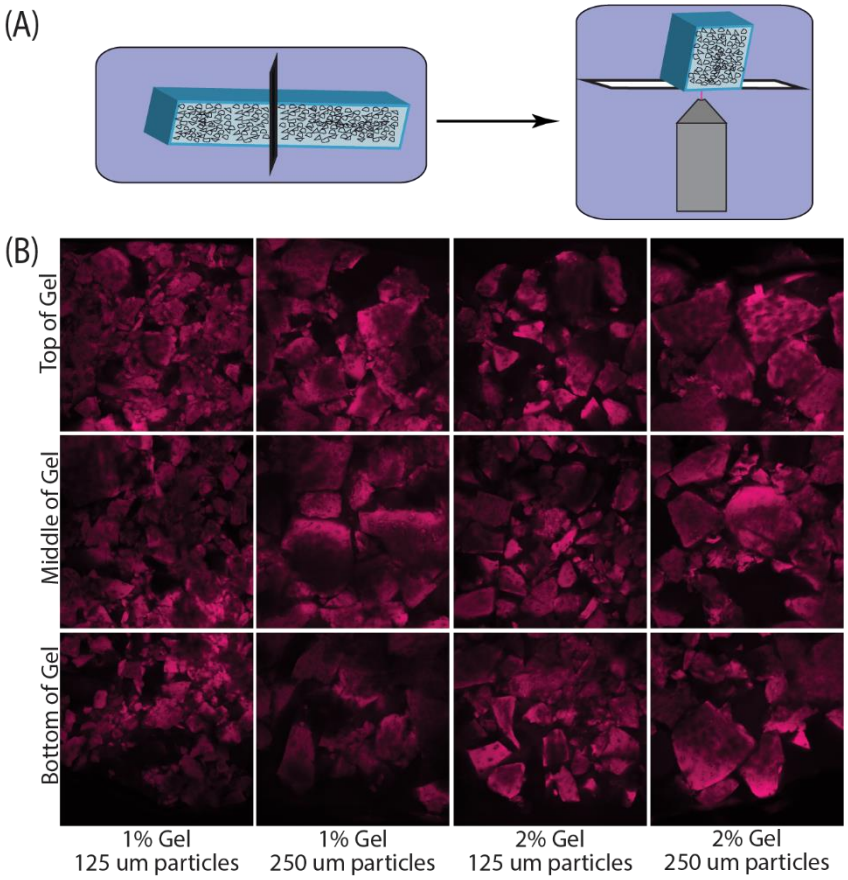

Figure S4. Particle packing was consistent throughout large volumes of the engineered materials. Tissue clays maintain the volume density of particles throughout the depth of the scaffold; **particles do not pack in higher density at the base of the scaffold due to settling**. (A) Polymerized scaffolds are bisected and imaged throughout the depth, (B) Particles of different sizes in HA/PEGDA gels of differing densities pack evenly throughout the depth of the scaffold.

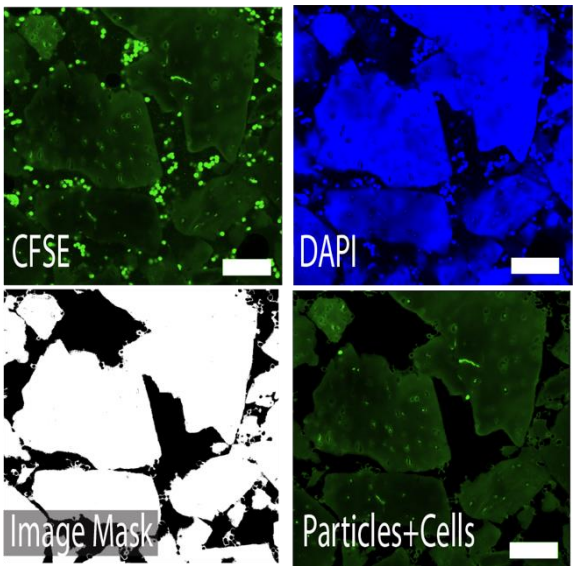

Figure S5. Custom Thresholding enabled quantification of the number of CFSE-stained cells that migrated into particles. Thresholding the particles using DAPI stain in the 405 nm channel allowed us to subtract the background. Once all cells in the hydrogel were subtracted from the background, particle measuring tools in ImageJ enabled quantification of CFSE stained cells in the particles at each time point. Scale Bar = 100µm.

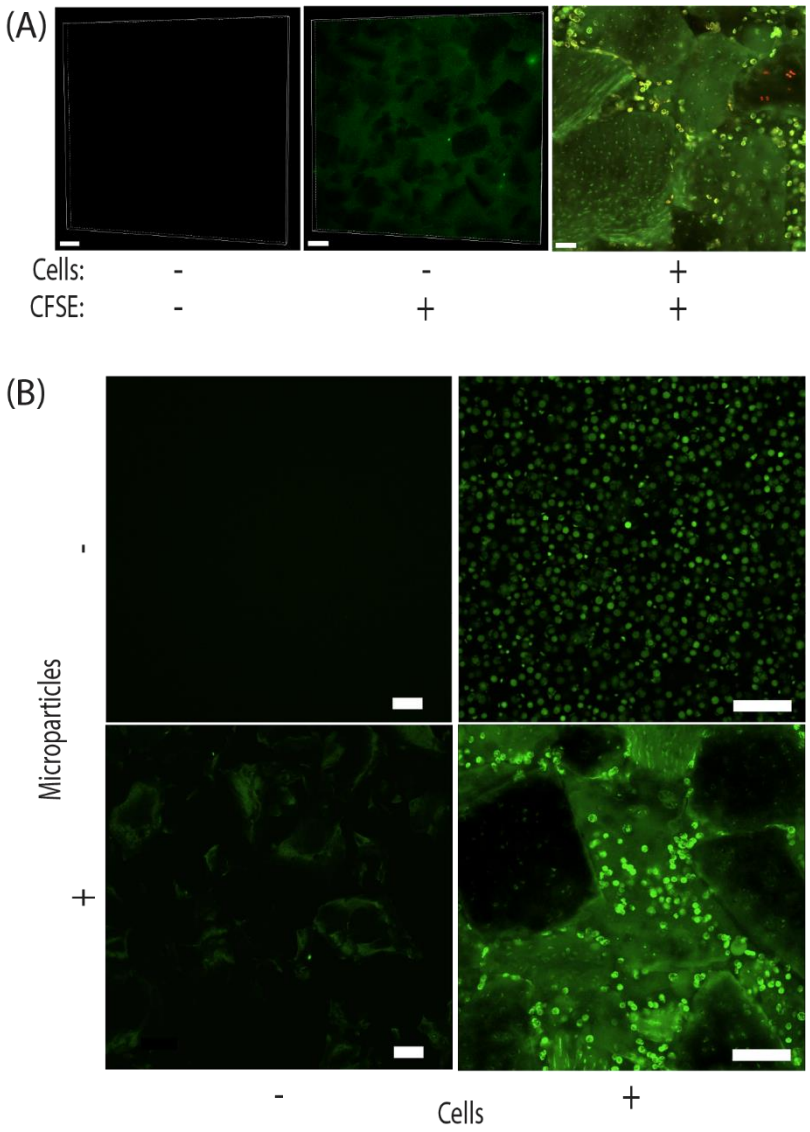

Figure S6. Images confirming CFSE staining of chondrocytes. (A) The addition of representative levels of CFSE to the microparticle gels does not show any bright localization to the particles. (B) Additionally, we do not observe staining due to imaging by confocal microscopy, or the microparticles alone, and we only observe a localization of signal with the addition of cells. Scale Bar = 100µm, final panel of (A), scale bar = 50µm.

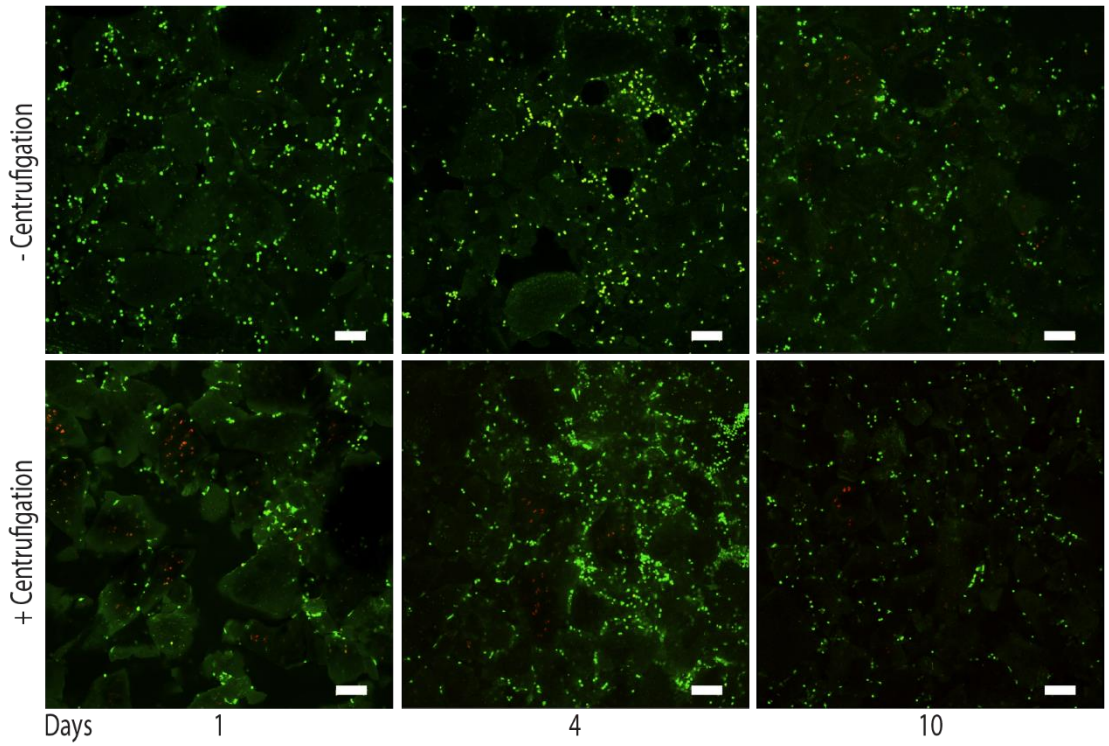

Figure S7. Post-centrifugation live/dead staining. Live dead staining of the cells before and after centrifugation (scaffold packing) demonstrates no dramatic increase in cell death. Green = Live cells, Red = Dead cells. Scale Bar = 100μm

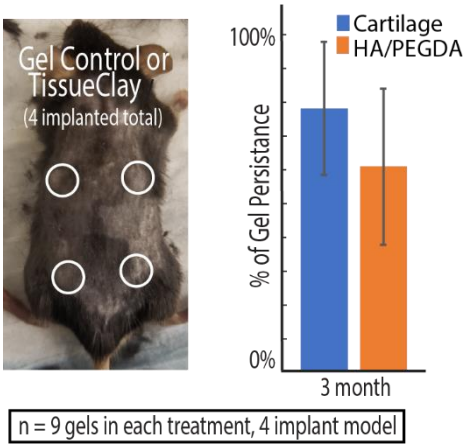

Figure S8. In a supplementary subcutaneous mouse study, we implanted 4 gels (2 *tissue clay* hydrogels and 2 HA/PEGDA controls) in 3 different mice (gel type randomized among the 4 highlighted locations). Data shown here represent the hydrogel persistence over 3 months and the trends agree with the persistence results reported in the main paper.

Supplementary Information References

[1] B. N. Brown, S. F. Badylak, in *Translating Regenerative Medicine to the Clinic*, **2015**.
[2] T. R. Cox, J. T. Erler, *DMM Disease Models and Mechanisms* **2011**, *4*, 165.
[3] R. Maroto, O. P. Hamill, *CHAPTER 17 MscCa Regulation of Tumor Cell Migration and Metastasis*, Elsevier Masson SAS, **2007**.
[4] K. Wolf, M. Te Lindert, M. Krause, S. Alexander, J. Te Riet, A. L. Willis, R. M. Hoffman, C. G. Figdor, S. J. Weiss, P. Friedl, *J Cell Biol* **2013**, *201*, 1069.
[5] C. M. Denais, R. M. Gilbert, P. Isermann, A. L. McGregor, M. Te Lindert, B. Weigelin, P. M. Davidson, P. Friedl, K. Wolf, J. Lammerding, *Science* **2016**, *352*, 353.
[6] F. Qu, Q. Li, X. Wang, X. Cao, M. H. Zgonis, J. L. Esterhai, V. B. Shenoy, L. Han, R. L. Mauck, *Scientific Reports* **2018**, *8*, 3295.
[7] Q. Li, C. Wang, B. Han, F. Qu, H. Qi, C. Y. Li, R. L. Mauck, L. Han, *J Biomech* **2018**, *72*, 252.
[8] S.-J. Heo, K. H. Song, S. Thakur, L. M. Miller, X. Cao, A. P. Peredo, B. N. Seiber, F. Qu, T. P. Driscoll, V. B. Shenoy, M. Lakadamyali, J. A. Burdick, R. L. Mauck, *Nuclear Softening Expedites Interstitial Cell Migration in Fibrous Networks and Dense Connective Tissues*, **2020**.
[9] T. Novak, K. F. Gilliland, X. Xu, L. Worke, A. Ciesielski, G. Breur, C. P. Neu, **n.d.**, DOI 10.1089/ten.tea.2016.0149.
[10] J. M. Silva Garcia, A. Panitch, S. Calve, *Acta Biomaterialia* **2019**, *84*, 169.
[11] K. L. Spiller, S. A. Maher, A. M. Lowman, *Tissue Eng Part B Rev* **2011**, *17*, 281.
[12] T. Novak, B. Seelbinder, C. M. Twitchell, S. L. Voytik-Harbin, C. P. Neu, *Advanced Functional Materials* **2016**, *26*, 5427.
[13] T. Novak, B. Seelbinder, C. M. Twitchell, C. C. van Donkelaar, S. L. Voytik-Harbin, C. P. Neu, *Advanced Functional Materials* **2016**, *26*, 2617.
[14] A. J. Sophia Fox, A. Bedi, S. A. Rodeo, *Sports Health* **2009**, *1*, 461.
[15] F. C. Linn, L. Sokoloff, *Arthritis & Rheumatism* **1965**, *8*, 481.
[16] C. Loebel, R. L. Mauck, J. A. Burdick, **n.d.**, DOI 10.1038/s41563-019-0307-6.
[17] M. N. Collins, C. Birkinshaw, *Carbohydrate Polymers* **2013**, *92*, 1262.
[18] Y. Chen, C. A. Schuh, *Journal of Statistical Physics* **2016**, *162*, 232.
[19] F. J. Vernerey, S. Bryant, *Current Opinion in Biomedical Engineering* **2020**, *15*, 68.
[20] A. A. Saberi, *Physics Reports* **2015**, *578*, 1.
[21] F. Qu, F. Guilak, R. L. Mauck, *Nature Reviews Rheumatology* **2019**.
[22] H. Akkiraju, A. Nohe, *Journal of developmental biology* **2015**, *3*, 177.
[23] P. M. Crapo, T. W. Gilbert, S. F. Badylak, *Biomaterials* **2011**, *32*, 3233.
[24] J. E. Reing, B. N. Brown, K. A. Daly, J. M. Freund, T. W. Gilbert, S. Hsiong, A. Huber, K. E. Kullas, S. Tottey, M. Wolf, S. F. Badylak, **n.d.**, DOI 10.1016/j.biomaterials.2010.07.083.
[25] B. N. Brown, S. F. Badylak, *Translational Research* **2014**, *163*, 268.
[26] D. Eng, M. Caplan, M. Preul, A. Panitch, *Acta Biomaterialia* **2010**, *6*, 2407.
[27] S. v. Plotnikov, A. M. Pasapera, B. Sabass, C. M. Waterman, *Cell* **2012**, *151*, 1513.
[28] J. Xue, A. He, Y. Zhu, Y. Liu, D. Li, Z. Yin, W. Zhang, W. Liu, Y. Cao, G. Zhou, *Biomedical Materials* **2018**, *13*, 025016.
[29] T. Novak, K. Fites Gilliland, X. Xu, L. Worke, A. Ciesielski, G. Breur, C. P. Neu, *Tissue Eng Part A* **2016**, *22*, 1274.
[30] C. R. Rowland, L. A. Colucci, F. Guilak, *Biomaterials* **2016**, *91*, 57.
[31] M. B. Albro, M. S. Bergholt, J. P. St-Pierre, A. Vinals Guitart, H. M. Zlotnick, E. G. Evita, M. M. Stevens, *npj Regenerative Medicine* **2018**, *3*, 3.
[32] Z. Movasaghi, S. Rehman, I. U. Rehman, *Applied Spectroscopy Reviews* **2007**, *42*, 493.

[33] A. Bonifacio, C. Beleites, F. Vittur, E. Marsich, S. Semeraro, S. Paoletti, V. Sergo, **n.d.**, DOI 10.1039/c0an00459f.
[34] E. Mariani, G. Lisignoli, R. M. Borzì, L. Pulsatelli, **2019**, DOI 10.3390/ijms20030636.
[35] G. Ofek, R. M. Natoli, K. A. Athanasiou, **n.d.**, DOI 10.1016/j.jbiomech.2009.01.024.
[36] N. Herzmann, A. Salamon, T. Fiedler, K. Peters, *Experimental Cell Research* **2016**, *342*, 95.
[37] A. J. Sutherland, G. L. Converse, R. A. Hopkins, M. S. Detamore, *Advanced Healthcare Materials* **2015**, *4*, 29.
[38] Z. Wang, Z. Li, Z. Li, B. Wu, Y. Liu, W. Wu, *Acta Biomaterialia* **2018**, *81*, 129.
[39] M. T. Wolf, K. A. Daly, E. P. Brennan-Pierce, S. A. Johnson, C. A. Carruthers, A. D'Amore, S. P. Nagarkar, S. S. Velankar, S. F. Badylak, *Biomaterials* **2012**, DOI 10.1016/j.biomaterials.2012.06.051.
[40] F. Pati, J. Jang, D.-H. Ha, S. Won Kim, J.-W. Rhie, J.-H. Shim, D.-H. Kim, D.-W. Cho, *Nature communications* **2014**, *5*, 3935.
[41] D.-A. Wang, S. Varghese, B. Sharma, I. Strehin, S. Fermanian, J. Gorham, D. H. Fairbrother, B. Cascio, J. H. Elisseeff, **2007**, DOI 10.1038/nmat1890.
[42] C. W. Cheng, L. D. Solorio, E. Alsberg, *Biotechnology Advances* **2014**, *32*, 462.
[43] L. K. Huang, M. J. J. Wang, *Pattern Recognition* **1995**, *28*, 41.
[44] K. M. Fischenich, J. A. Wahlquist, R. Wilmoth, L. Cai, C. P. Neu, V. L. Ferguson, *Osteoarthritis and Cartilage* **2020**, 1.
[45] Nih, Od, Oer, Olaw, *Guide for the Care and Use of Laboratory Animals*, **2011**.
[46] Y. Mishima, M. Lotz, *Journal of Orthopaedic Research* **2008**, *26*, 1407.
[47] F. Qu, J. L. Holloway, J. L. Esterhai, J. A. Burdick, R. L. Mauck, **n.d.**, DOI 10.1038/s41467-017-01955-w.
[48] S. Corti, S. Salani, R. Del Bo, M. Sironi, S. Strazzer, M. G. D'Angelo, G. P. Comi, N. Bresolin, G. Scarlato, *Experimental Cell Research* **2001**, DOI 10.1006/excr.2001.5267.
[49] H. Bergmeister, C. Schreiber, C. Grasl, I. Walter, R. Plasenzotti, M. Stoiber, D. Bernhard, H. Schima, **2013**, *9*, 6032.
[50] A. M. Greiner, M. Jäckel, A. C. Scheiwe, D. R. Stamow, T. J. Autenrieth, J. Lahann, C. M. Franz, M. Bastmeyer, *Biomaterials* **2014**, *35*, 611.
[51] C. M. Denais, R. M. Gilbert, P. Isermann, A. L. McGregor, M. Te Lindert, B. Weigelin, P. M. Davidson, P. Friedl, K. Wolf, J. Lammerding, *Science* **2016**, *352*, 353.
[52] S. Even-Ram, K. M. Yamada, *Current Opinion in Cell Biology* **2005**, *17*, 524.
[53] E. Cukierman, R. Pankov, D. R. Stevens, K. M. Yamada, *Science* **2001**, *294*, 1708.
[54] H. Schöndorf, H. Naujoks, *Journal of cancer research and clinical oncology* **1985**, *109*, 241.
[55] G. Maheshwari, H. Steven Wiley, D. A. Lauffenburger, *The Journal of Cell Biology* **2001**, *155*, 1123.
[56] H. Pereira, S. G. Caridade, A. M. Frias, J. Silva-Correia, D. R. Pereira, I. F. Cengiz, J. F. Mano, J. M. Oliveira, J. Espregueira-Mendes, R. L. Reis, *Osteoarthritis and cartilage / OARS, Osteoarthritis Research Society* **2014**, DOI 10.1016/j.joca.2014.07.001.
[57] M. A. Morrissey, D. R. Sherwood, *Journal of Cell Science* **2015**, *128*, 1661.
[58] S. R. Peyton, A. J. Putnam, *Journal of Cellular Physiology* **2005**, *204*, 198.
[59] A. Otto, H. Collins-Hooper, A. Patel, P. R. Dash, K. Patel, *Rejuvenation Research* **2011**, *14*, 249.
[60] A. J. Sophia Fox, A. Bedi, S. A. Rodeo, *Sports health* **2009**, *1*, 461.
[61] G. D. O'Connell, A. R. Tan, V. Cui, J. C. Bulinski, J. L. Cook, M. Attur, S. B. Abramson, G. A. Ateshian, C. T. Hung, *Journal of Tissue Engineering and Regenerative Medicine* **2017**, *11*, 877.

[62] N. Herzmann, A. Salamon, T. Fiedler, K. Peters, *Experimental Cell Research* **2016**, DOI 10.1016/j.yexcr.2016.03.016.
[63] Y.-X. Qin, W. Lin, C. Rubin, **2002**, DOI 10.1114/1.1483863.
[64] E. D. Hay, *Acta Anatomica* **1995**, *154*, 8.
[65] C. W. Patrick, **2004**, DOI 10.1146/annurev.bioeng.6.040803.140032.
[66] Y. C. Choi, J. S. Choi, B. S. Kim, J. D. Kim, H. I. Yoon, Y. W. Cho, **n.d.**, DOI 10.1089/ten.tec.2012.0009.
[67] M. Bajénoff, J. G. Egen, H. Qi, A. Y. C. Huang, F. Castellino, R. N. Germain, *Trends in Immunology* **2007**, *28*, 346.